

1 **Comparisons of Daily Sea Surface Temperature**
2 **Analyses for 2007-2008**

3
4
5 Richard W. Reynolds
6 NOAA National Climatic Data Center, Asheville, North Carolina

7
8 Dudley B. Chelton
9 College of Oceanic and Atmospheric Sciences and Cooperative Institute for Oceanographic
10 Satellite Studies, Oregon State University, Corvallis, Oregon
11
12

13
14
15
16
17
18
19
20
21
22
23
24
25
26

27 _____
28
29 Corresponding author address: Richard W. Reynolds. NOAA's National Climatic Data Center,
30 151 Patton Avenue, Asheville, NC, 28801-5001
31 E-mail: Richard.w.reynolds@noaa.gov

1 **Abstract**

2
3

4 Six different SST analyses are compared with each other and with buoy data for the
5 period: 2007-2008. All analyses used different combinations of satellite data (for example
6 infrared Advanced Very High Resolution Radiometer, AVHRR, and microwave Advanced
7 Microwave Scanning Radiometer, AMSR, instruments) with different algorithms, spatial
8 resolution, etc. The analyses considered are: the National Climatic Data Center (NCDC)
9 AVHRR-only and AMSR+AVHRR, the Navy Coupled Ocean Data Assimilation (NCODA), the
10 Remote Sensing Systems (RSS), the Real Time Global High Resolution (RTG- HR) and the
11 Operational SST and Sea Ice Analysis (OSTIA); the spatial grid sizes were $1/4^\circ$, $1/4^\circ$, $1/9^\circ$,
12 $1/11^\circ$, $1/12^\circ$ and $1/20^\circ$, respectively. In addition, all analyses except RSS used in situ data. Most
13 analysis procedures and weighting functions differed. Thus, differences among analyses could
14 be large in high gradient and data sparse regions. An example off the coast of South Carolina
15 showed winter SST differences that exceeded 5°C .

16 To help quantify SST analysis differences, wavenumber spectra were computed at several
17 locations. These results suggested that the RSS is much noisier and that the RTG-HR analysis is
18 much smoother than the other analyses. Further comparisons made using collocated buoys
19 showed that RSS was especially noisy in the tropics and that RTG-HR had winter biases near the
20 Aleutians Region during January and February 2007. The correlation results show that NCODA,
21 and to a somewhat lesser extent, OSTIA are strongly tuned locally to buoy data. The results also
22 show that grid spacing does not always correlate with analysis resolution.

23 The AVHRR-only analysis is useful for climate studies because it is the only daily SST
24 analysis that extends back to September 1981. Furthermore, comparisons of the AVHRR-only

1 analysis and the AMSR+AVHRR analysis show that AMSR data can degrade the combined
2 AMSR and AVHRR resolution in cloud-free regions while AMSR otherwise improves the
3 resolution. These results indicate that changes in satellite instruments over time can impact SST
4 analysis resolution.

5

1. Introduction

Sea surface temperature (SST) analyses are useful for many purposes including hurricane forecasting, fisheries operations, air sea flux studies, as the ocean surface boundary condition for atmospheric models and for studies of climate change and prediction. In recent years the number of satellite instruments has increased. This has helped facilitate an increase in the number of additional data and analysis products that are operational or under development. Many of these products are produced by the Group for High-Resolution Sea Surface Temperature (GHRSSST) (see Donlon et al. 2007, and <http://www.ghrsst-pp.org/>, see in particular "Data Access"). GHRSSST products are used for many purposes (see publication list at <http://www.ghrsst-pp.org/Peer-reviewed-articles.html>.) The analyses use in situ and remotely sensed data from a variety of geostationary and polar-orbiting satellites and are computed over different regions and time periods with different spatial and temporal resolutions. Users now have a choice of analyses that was never possible before GHRSSST was established. Most of these products tend to cover roughly the last five years when satellite instruments such as the microwave (MW) Advanced Microwave Scanning Radiometer (AMSR) and the infrared (IR) Moderate Resolution Imaging Spectroradiometer (MODIS), joined two longer time series of IR instruments as sources of global SST observations: the Advanced Very High Resolution Radiometer (AVHRR), since November 1981, and the Along Track Scanning Radiometer (ATSR), since August 1991.

The problem for users is not to obtain an SST analysis but to choose among the many that are available the one that is best suited to their particular purpose. Every analysis is designed to produce a regularly gridded product from irregularly spaced data. Most SST analyses use

1 statistical techniques to produce gridded products without dynamical considerations. Analyses
2 can be produced at any temporal interval for any spatial grid. As the resolution increases, the
3 signal may increase depending on the resolution of the data. However, as the resolution
4 increases, the noise also increases. The bottom line is that no analysis works when there are no
5 observations nearby in space and/or time. Of course as more high resolution satellite data
6 become available, the analysis resolution can be increased. With presently available data,
7 differences among daily analyses are larger than differences among monthly analyses, and the
8 daily differences can exceed 5°C, as will be discussed below.

9 The details of the design of each analysis vary. One of the first choices is which SST data
10 should be used in the analysis procedure. Then choices have to be made on the spatial grid
11 spacing and the update frequency of the analysis. Next, bias corrections need to be considered
12 along with analysis parameters such as error correlation scales and the signal-to-noise ratios.
13 These and other choices that must be considered in the design of an analysis procedure may lead
14 to very different results. For example, SST observations which exceed some predetermined
15 threshold are often discarded. Thus, observations near this threshold are either kept or discarded
16 based on small differences.

17 In this paper, six different analyses are compared for the 2007-2008. The results
18 produced here may have to be reevaluated in the future as the accuracy and resolution of
19 analyses evolve as satellite instruments change and as improvements in analysis procedures are
20 implemented. The most useful result of this comparison is to identify problems in the various
21 analyses, which will hopefully lead to improvements.

22

1 **2. Overviews of the Six SST Analysis Products**

2 Analyses were selected that were global with at least daily resolution and available for
3 the two year period, 2007-2008. The minimum requirement of 2 years eliminates several newer
4 analyses but allows comparisons over a substantial time period. Five analyses meeting the
5 requirements were selected from the GHRSSST Global Data Assembly Center (GDAC) at the JPL
6 Physical Oceanography Distributed Active Archive Center (PO.DAAC) (see table at
7 http://ghrsst.jpl.nasa.gov/GHRSSST_product_table.html). One additional analysis from the
8 National Oceanic and Atmospheric Administration's (NOAA) National Centers for
9 Environmental Prediction (NCEP) was added because it is presently used operationally in two
10 forecast models: the regional North American Mesoscale (NAM) model at NCEP (Thiébaux et
11 al. 2003) and the global forecast model at the European Centre for Medium-Range Weather
12 Forecasts (ECMWF) (Chelton and Wentz, 2005). All analyses can be obtained from
13 <ftp://podaac.jpl.nasa.gov/pub/GHRSSST/data/L4/GLOB/> unless specifically noted below. The
14 analyses are discussed in order of increasing grid spacing and summarized in Table 1. GHRSSST
15 (Donlon et al. 2007) recommends that analyses be produced at the foundation temperature,
16 defined as the temperature at the shallowest depth below any diurnal variations.

17 There are several sources of in situ and AVHRR data. For the period considered here, the
18 in situ SST data are from ships and buoys and collected over the real time Global
19 Telecommunication System (GTS); the AVHRR data are from the US Navy (May et al. 1998).
20 This AVHRR algorithm separately corrects daytime and nighttime satellite data with collocated
21 buoy data.

22

1 a. *AVHRR-only and AMSR+AVHRR Analyses*

2 Two of the analyses are produced daily on a $1/4^\circ$ grid at NOAA's National Climatic Data
3 Center (NCDC) as described by Reynolds, et al. (2007). One analysis (AVHRR-only) uses in
4 situ and AVHRR data. The second analysis (AMSR+AVHRR) adds AMSR data. Both analysis
5 procedures are the same. In situ data from ships and buoys are used to provide a large-scale bias
6 correction of the satellite data. All data are used for a given day, where the day is defined by
7 Coordinated Universal Time (UTC). However, the satellite data are separated into daytime and
8 nighttime bins and corrected separately using all in situ data. Then the in situ and corrected
9 satellite data are analyzed using an optimum interpolation (OI) procedure. These two analyses
10 were computed to determine the impact of an analysis variance jump when AMSR became
11 available in June 2002. The error correlation scales range from 50-200 km with smaller scales at
12 higher latitudes (especially in western boundary current regions) and larger scales in the tropics.

13 Version 2 of the OI procedure, as described by Reynolds et al. (2007), is used here. The
14 changes from version 1 are relatively small and primarily consist of additional temporal
15 smoothing. The temporal smoothing includes using 3 consecutive days of data, with the middle
16 day weighted higher than the other two days. The date of the analysis is defined to be the middle
17 day of each 3-day analysis period. The temporal smoothing also includes additional smoothing of
18 the bias corrections which tend to be noisy due to limited in situ observations. In addition, ship
19 SSTs are corrected relative to the buoy SSTs by subtracting 0.14°C from all ship observations
20 before they are used to bias correct the satellite data. Thus, all observations are bias corrected
21 with respect to buoy SSTs and there are no corrections to foundation temperature. The changes
22 in version 2 are described in more detailed in

1 <http://www.ncdc.noaa.gov/oa/climate/research/sst/papers/whats-new-v2.pdf>. Additional up-to-
2 date information is available at <http://www.ncdc.noaa.gov/oa/climate/research/sst/oi-daily.php>.

3

4 *b. NCODA Analysis*

5 The US Navy Coupled Ocean Data Assimilation (NCODA) analysis (Cummings, 2005)
6 is computed operationally using in situ data and AVHRR data. In addition to the ship and buoy
7 SST in situ data used by other analyses, the NCODA analysis also includes in situ hydrographic
8 temperature and salinity profiles.

9 The analysis is performed on a $1/9^\circ$ grid on the equator with gradual reductions in
10 latitudinal intervals to keep the size of the grid boxes nearly equal area between 80°S and 80°N .
11 The NCODA analysis is done every 6 hours using data within ± 3 hours of the date of the
12 analysis. However, NCODA has a floating "look back time" for every instrument to ensure that
13 all data get into the analysis (Cummings, personal communication, 2009). Because of this
14 potential delay, incoming data may not be centered on the analysis time window. No bias
15 correction of satellite data is performed. However, diurnal warming events are flagged and some
16 flagged observations may be eliminated in light winds. The error correlation scales are
17 determined by the Rossby radius of deformation obtained from Chelton et al. (1998) and range
18 from ~ 10 km near the pole to ~ 220 km at the equator. As described in Cummings (2005),
19 NCODA is implemented as the data assimilation component of the Hybrid Coordinate Ocean
20 Model (for details see <http://www.hycom.org/dataserver/glb-analysis/expt-90pt8>). In this
21 assimilation system altimeter data and atmospheric forcing fields are also used. NCODA is the
22 only analysis considered here that is linked to a dynamical model. All the other analyses are
23 statistical analyses only. NCODA therefore has a strong potential advantage if the ocean

1 dynamics from the model are realistic. Analyses from July 2005 to present are available from
2 <http://usgodae2.fnmoc.navy.mil/ftp/outgoing/fnmoc/models/ghrsst/>; the JPL web site has
3 analyses beginning in April 2008.

4 *c. RSS Analysis*

5 The Remote Sensing Systems (RSS) analysis is computed on a $\sim 1/11^\circ$ grid using AMSR,
6 Tropical Rainfall Measuring Mission Microwave Imager (TMI) and MODIS data. The analysis
7 uses 3-days of consecutive data with the analysis date referenced by the middle day. The
8 analysis has a constant error correlation scale of 1.5° (~ 165 km on the equator) and is the only
9 analysis that does not use in situ data directly. There is no correction for a foundation
10 temperature. However, AMSR and TMI retrievals are calibrated and validated by buoys.
11 Furthermore, large-scale MODIS biases are removed by adjustment to AMSR. All observations
12 are adjusted to remove any diurnal signal based on the local time of day and wind speed,
13 following Gentemann et al. (2003). This analysis is not yet published (Gentemann, 2009,
14 personal communication), although some details are available at
15 http://www.ssmi.com/sst/microwave_oi_sst_browse.html.

16
17 *d. NCEP RTG-HR Analysis*

18 The NCEP Real Time Global High Resolution (RTG-HR) is operationally computed
19 daily using in situ and AVHRR data on a $1/12^\circ$ grid. The analysis is computed at 0000 UTC
20 using observations within ± 12 hours. The analysis has no diurnal correction or depth adjustment
21 to foundation temperature. The error correlation scales range from 50 to 450 km based on the
22 climatological SST gradients with smaller (larger) scales related to larger (smaller) gradients (see

1 Thiébaux et al. 2003). The satellite data are corrected relative to the in situ data following the
2 Poisson scheme of Reynolds and Smith (1994). This version is described by the unpublished
3 manuscript Gemmill et al. (2007), which is available from <http://polar.ncep.noaa.gov/sst/> along
4 with other analysis details. Only the most recent year of analyses is available for download at
5 <ftp://polar.ncep.noaa.gov/pub/history/sst/ophi/>. The RTG-HR analysis is not part of the GHRSSST
6 program and so is not available from the GDAC. Thiébaux et al. (2003) describe the earlier
7 version of this analysis on a coarser grid (see also Chelton and Wentz, 2005).

8

9 *e. U.K. Met Office OSTIA Analysis*

10 The UK Met Office produces an Operational SST and Sea Ice Analysis (OSTIA) on a
11 $1/20^\circ$ grid that uses in situ, AVHRR, AMSR, TMI, Advanced ATSR (AATSR), and
12 geostationary Spinning Enhanced Visible and Infrared Imager (SEVIRI) data. The analysis is run
13 daily at 0600 UTC using data from a 36 hour period ending at 0600 using two error correlation
14 scales, 10 and 100 km, which vary depending on the region and the input data. To produce a
15 foundation temperature, the input data are then filtered to remove daytime observations with
16 wind speed < 6 m/s which may contain diurnal surface warming. All satellite SST data are
17 adjusted for bias errors by reference to a combination of AATSR and in situ SST measurements
18 from drifting buoys. Further details can be found in Donlon et al. (2009) and at
19 http://ghrsst-pp.metoffice.com/pages/latest_analysis/ostia.html.

20

21 *f. Some General Comments*

22 It is important to point out that all the analyses except the NCODA have some type of
23 satellite bias correction using either in situ data or one type of satellite data (or both in the case of

1 OSTIA) as a reference. If this is not done, small biases may lead to jumps as data are contributed
2 by different satellite instruments. Reynolds et al. (2010) show that this bias occurs (see in
3 particular Figs. 4 and 5) even for two different nighttime AVHRR instruments using the same
4 algorithms.

5 Only the RSS analysis specifically corrects the data to remove the diurnal cycle. This
6 removal may lead to errors because accurate information on the surface heat fluxes is needed for
7 accurate estimates of the diurnal cycle. However, such information is not available for use in the
8 RSS analysis procedure. In OSTIA and NCODA, there are adjustments to remove some diurnal
9 signal by deleting daytime observations in low winds. The other analyses bias correct satellite
10 data to match spatially and temporally averaged in situ data in an effort to reduce the impact of
11 diurnal warming.

12

13 **3. Qualitative differences**

14 Qualitative comparisons of SST maps from the various products show areas with large
15 differences (exceeding several °C) during the two-year time period 2007-2008 considered here.
16 The regions with the largest differences tend to occur near the coast, in strong gradient regions
17 such as western boundary currents and at high latitudes where SST measurements (both in situ
18 and satellite) tend to be sparse. In addition, SSTs are simulated in some of the analyses based on
19 sea-ice concentrations (see Reynolds, et al. 2007, for details), which may contribute to the
20 differences among analyses at high latitudes.

1 Figure 1 shows regional SST fields off the Carolina Coast for 1 January 2007. This
2 region was selected because the warm Gulf Stream is found off shore in winter while colder shelf
3 water is present between the Gulf Stream and the coast. The shelf water cannot be detected by
4 MW retrievals because it is too near the coast where MW observations are contaminated by land
5 in the antenna sidelobes. Furthermore, winter clouds can limit IR retrievals. The detection of the
6 shelf water is especially difficult off the South Carolina Coast because there are no moored
7 buoys there. Thus, it will sometimes be difficult to detect the shelf water in statistical-only
8 analyses. In Fig. 1, the colder shelf water is evident in the AVHRR-only, the AMSR+AVHRR,
9 the NCODA and the RTG-HR analyses, but is partly missing in the RSS and the OSTIA
10 analyses. In addition, the small-scale variability is highest in the RSS analysis and lowest in
11 RTG-HR and OSTIA.

12 Figure 2 shows the SST gradient magnitudes for the same region and time as in Fig. 1.
13 The SST gradients associated with the Gulf Stream are clearest off the Carolinas in NCODA and
14 weakest in RSS and OSTIA. The gradients in the AVHRR-only and AMSR+AVHRR analyses
15 are not as clear adjacent to the coast because of the relatively coarse $1/4^\circ$ grid compared with the
16 grid spacing of the other analyses; the gradients were computed with centered differences only if
17 all east-west and north-south nearest grid values were ocean values. North of about 35°N , the
18 gradients in the AVHRR-only and the AMSR+AVHRR sharpen and become very sharp in the
19 RSS.

20 It is noteworthy that the gradients north of 35°N are actually a little sharper in the
21 AVHRR-only analysis than in the AMSR+AVHRR analysis. The AVHRR and AMSR data were
22 gridded on the same $1/4^\circ$ grid in the AVHRR-only and AMSR+AVHRR analyses. However, the

1 AMSR data resolution is only about 50 km while the AVHRR data resolution is 4-9 km. Thus,
2 AMSR data slightly reduced the gradients in this case. However, in cloud covered regions further
3 off the coast, AVHRR observations become sparse and the AMSR can improve the analysis
4 resolution relative to AVHRR-only (see Reynolds et al. 2007, Fig. 9).

5 Figure 3 shows SST fields for a region in the western tropical Pacific for 1 January 2007.
6 SST variability and gradients are small in this region. In addition, SST temperatures between
7 10°S and 10°N are near 30°C, as shown in the figure, with abundant rainfall year-round due to
8 strong convective activity. Thus, IR satellite retrievals are limited by cloud cover and to a lesser
9 extent MW satellite retrievals are limited by precipitation. The results show that the features are
10 smoothest in the RTG-HR analysis. The RSS analysis has considerable small-scale structure that
11 apparently arises from inclusion of 1-km data from MODIS. However, because MODIS data are
12 limited by swath width and clouds, they are not available every day for the region shown in the
13 figure. Thus, some of the RSS small scale details may arise from conditions several days earlier
14 and persistence in the RSS analysis procedure.

15 Figure 4 shows the SST gradient magnitude off the west coast of the U.S. for 1
16 September 2008, a time of year when coastal upwelling is generally strong. Upwelling is evident
17 along the coasts of Oregon, Washington and Northern California from the narrow band of strong
18 SST gradients adjacent to the coast. The strong and meandering SST gradients farther offshore
19 are frontal regions associated with eddies and meanders of the California Current (Castelao et al.
20 2006). The SST gradients are strongest in the NCODA analysis. The coastal gradients are
21 somewhat weaker in OSTIA and even weaker in the AMSR+AVHRR and AVHRR-only
22 analyses. The coastal gradients are the weakest and SST gradients are almost nonexistent in the

1 open-ocean regions offshore. RSS shows very strong and fine-scale SST gradients nearshore.
2 However, the SST gradients are again very noisy everywhere in the RSS analysis.

3

4 **4. Wavenumber spectra**

5 The feature resolutions of the six SST analysis products considered in this study are
6 evident from the zonal wavenumber spectra in Fig. 5. Spectra are shown for a Southern
7 Hemisphere mid-latitude region (the Agulhas Return Current, ARC, in the South Indian Ocean),
8 a Northern Hemisphere mid-latitude region (the Kuroshio Extension, KE, in the North Pacific
9 Ocean), and the Western Tropical Pacific (WTP). Each spectrum is the ensemble average of 31
10 individual zonal wavenumber spectra computed from daily SST fields over the months of
11 January 2007 and July 2007.

12 A consistent feature in all six panels of Fig. 5 is that the RSS SST fields have much
13 higher spectral energy than any of the other SST products at wavelengths shorter than about 300
14 km. The RSS spectra roll off with zonal wavenumber, k , as approximately k^{-2} in all cases. In
15 comparison, the wavenumber dependence of the OSTIA spectra ranges from k^{-4} to k^{-5} . The
16 NCODA, AVHRR-only and AMSR+AVHRR spectra are somewhat steeper. The spectral energy
17 in the RSS fields is more than 2 orders of magnitude higher than any of the other SST analyses at
18 the highest wave numbers. The existence of a k^{-2} spectrum is not in general an indication of noise
19 in the data. However, the fundamentally different spectral behavior of the RSS SST fields
20 compared to the other SST analyses and the noisy, "speckled", appearance of the RSS SST fields
21 in Figs. 2-4, is a clear indication that the RSS fields are dominated by small-scale noise. It should

1 also be noted that the k^{-2} falloff is also evident at the shortest wavelengths in the ARC region in
2 all analyses except the OSTIA. The k^{-2} falloff at these short scales may be interpreted as an
3 indication of ‘red’ noise in all the analyses except OSTIA, rather than an abrupt change in the
4 spectral characteristics of SST at short wavelengths.

5 Another consistent feature in all six panels of Fig. 5 is that the RTG-HR SST fields have
6 significantly lower feature resolution than any of the other SST products, as evident from the
7 steep roll off of the spectra at wavelengths shorter than about 250 km in the ARC and KE
8 regions. This roll off indicates that the analysis procedure evidently attenuates the variability
9 with scales shorter than about 250 km. In the two mid-latitude regions, the RTG-HR spectra are
10 very similar to the other spectra at wavelengths longer than about 250 km. The RTG-HR SST
11 fields are characterized by a red noise with roughly k^{-3} spectral rolloff that extends to quite long
12 wavelengths of about 150 km in the ARC and KE and more than 500 km in the WTP. This is
13 presumably due to spatial smoothing of noisy SST fields as part of the RTG-HR analysis
14 procedure.

15 In the WTP region, the spectral rolloff of the NCODA SST fields is approximately k^{-4} at
16 wavelengths shorter than about 750 km, indicating that NCODA attenuates signals with these
17 scales. As a result, the NCODA variance at wavelengths shorter than about 250 km in January
18 and about 150 km in July is smaller than the $\sim k^{-3}$ noise variance in the RTG-HR fields. As a
19 result, RTG-HR has the illusion of having higher resolution than NCODA. It would be risky to
20 interpret these shorter-scale features as real in the RTG SST fields, given the approximate k^{-3} red
21 spectral characteristics of the noise that evidently exists in the RTG fields.

1 The wavenumber spectral analysis thus identifies important problems in the RSS and
2 RTG-HR SST products in all three of the regions considered here and the NCODA product in the
3 WTP region. The differences between the spectra of the other SST products are more subtle, but
4 some generalizations can nonetheless be made. In all six panels of Fig. 5, the OSTIA SST
5 analyses have consistently more energy than AVHRR-only, AMSR+AVHRR and NCODA at
6 wavelengths shorter than about 200 km; the differences approach an order of magnitude in some
7 cases. This higher energy may be an indication that the OSTIA analysis procedure utilizes the
8 information content of the IR measurements more effectively than the other analyses.

9 In the two mid-latitude regions, the spectra of the NCODA SST analyses are very similar
10 to the other SST products for wavelengths longer than about 150-200 km but have a steeper
11 spectral rolloff of $\sim k^{-4}$ at shorter wavelengths. As noted above, the underestimation of the
12 spectral energy at short scales in NCODA is much worse in the WTP, where the discrepancy is
13 more than an order of magnitude in July 2007 and nearly 3 orders of magnitude in January 2007.
14 The steepness and linearity of the roll offs of the NCODA spectra, and the visually smooth
15 appearance of the NCODA SST fields in Fig. 3, strongly suggest that the NCODA SST analyses
16 are overly smooth in all three of the open-ocean regions considered in these wavenumber
17 spectral analyses. This contrasts with the high resolution of the NCODA analysis that is visually
18 apparent in the California Current region (Fig. 4). The NCODA analysis procedure for open-
19 ocean regions thus apparently utilizes the IR measurements less effectively than the other
20 analyses except for RTG-HR.

21 The differences between the AVHRR-only and AMSR+AVHRR SST analyses in Fig. 5
22 are surprising. The AMSR+AVHRR spectral energy at the higher wave numbers is significantly

1 less in the midlatitude regions during the summertime (January in the ARC and July in the KE)
2 and slightly less in the WTP during January. Although the summertime differences are not great,
3 it may be counterintuitive that the AVHRR-only fields have more small-scale energy than the
4 AMSR+AVHRR fields. This difference is likely attributable to the greater prevalence of
5 AVHRR data in the summertime in the ARC and KE and during January in the WTP because of
6 reduced cloudiness, which allows accurate mapping of the SST field without inclusion of AMSR
7 data. Inclusion of the much coarser ~50 km resolution AMSR data at these times of prevalent
8 AVHRR data evidently results in a smoothing of the SST fields that would otherwise be obtained
9 from the ~25 km resolution AVHRR data alone. (The AVHRR data are degraded to the grid
10 spacing, $1/4^\circ$ or ~ 25 km, in the AVHRR-only analysis.)

11 In the three regions considered here, the differences between the AVHRR-only and
12 AMSR+AVHRR thus suggest that the AMSR observations do not contribute much additional
13 information beyond what can be obtained from AVHRR data alone, and in fact can be
14 detrimental to the resolution of SST analyses during times of good AVHRR coverage. This result
15 provides a very encouraging assessment of the accuracy of the long record of AVHRR-only
16 fields that date back to September 1981, long before the availability of all-weather microwave
17 observations of SST from TMI (since December 1997) and AMSR (since June 2002). However,
18 on a daily basis AMSR provides the only SST retrievals in persistently cloud-covered regions.
19 This is clearly shown in the better resolution of AMSR+AVHRR over AVHRR-only in the Gulf
20 Stream in Fig. 9 from Reynolds et al. (2007).

21

22 **5. Comparisons with Buoy Data**

1 To further quantify these results, comparisons were carried out using buoy data that were
2 gridded onto a $1/4^\circ$ grid and quality controlled to eliminate extreme SST values. As noted above,
3 buoys are used in all analyses except the RSS analysis. Thus, the buoys are not independent data.
4 The extent to which the buoy SSTs were replicated in any particular SST product depends on
5 how heavily they were weighted compared to the satellite and other in situ data used in the
6 analysis procedure.

7 SST observations from drifting and moored buoys are typically made by a thermistor or
8 hull contact sensor and usually are obtained in real time by satellites. Although the accuracy of
9 the buoy SST observations varies, the random error is usually smaller than 0.5°C . Further
10 information on buoy data is available from McPhaden et al. (1988) and Bourlès et al. (2008).

11

12 *a. Buoy Data*

13 Over the 2007-2008 period, the gridded buoy data were screened for locations with at
14 least one daily observation for 90% of the days (658 days out of 731). The resulting 92 locations
15 are shown in Fig. 6 where the data are grouped into the ten regions shown. (If a 95% threshold
16 were used, the number of buoy locations dropped to 81. The 95% threshold especially affected
17 the Eastern Tropical Pacific Region where locations east of 120°W were missing altogether).
18 Both moored and drifting buoy data were used. However, because of the temporal coverage
19 restrictions, almost all of the data were from moored buoys. A typical distribution of moored and
20 drifting buoy data can be seen in Fig. 1 of Reynolds et al. (2002) and the most recent weekly

1 distribution is available from
2 http://www.emc.ncep.noaa.gov/research/cmb/sst_analysis/images/inscol.png.

3 It should be noted that these buoy data are real-time GTS observations. The number of
4 moored tropical Pacific (<http://www.pmel.noaa.gov/tao/>) and tropical Atlantic
5 (<http://www.pmel.noaa.gov/pirata/>) buoy observations are denser when delayed observations are
6 included. Figure 6 indicates the location of 0.25° grid boxes within which the daily return from
7 the buoys was at least 90%. Mooring locations may vary with time for several reasons.
8 Depending on their design they may move within a watch circle with a radius of a few
9 kilometers, and they may also move farther when pulled on by fishermen. In addition, the
10 location may change by several kilometers or more when buoys are replaced with new moorings.
11 This variation in location resulted in data from some mooring sites being spread between two or
12 more 0.25° grid cells over the 2-year period, thus reducing the data return.

13 Time series from each of the six SST analyses were constructed by spatial linear
14 interpolation to the buoy locations. Missing data in all time series (both data and analysis) were
15 filled by temporal linear interpolation. In the results that follow, statistics were computed at each
16 buoy location and then averaged over each region.

17

18 *b. Regional Biases*

19 To examine the large-scale regional biases, differences between monthly averages of the
20 buoys and each of the analyses were computed at each buoy location (Fig. 6). The monthly
21 differences were averaged over the region to produce a regional monthly bias. The final step was

1 to compute the RMS of the regional monthly biases for the 24 months in 2007-2008. RMS
2 values were used rather than a simple average to avoid any possible impact of alternating signs in
3 lowering the final bias estimates.

4 RMS values of the monthly regional biases are shown in Fig. 7. In almost all regions,
5 RSS shows the largest biases, and RTG-HR has the second largest biases, while NCODA has the
6 lowest bias. The biases are generally smaller in the tropical regions than the higher latitude
7 regions. The climatological SST standard deviation from the International Comprehensive
8 Ocean–Atmosphere Dataset (ICOADS: e.g., Worley et al. 2005) increases from the tropics
9 (roughly 1°C) to the Gulf Stream (roughly 3°C). Thus, the latitudinal variation of the bias in Fig.
10 7 should be expected. Four areas stand out as having the largest overall biases: the three Gulf
11 Stream Regions and the Aleutians Region. In the three Gulf Stream Regions, the RSS clearly has
12 the largest biases, especially in the region off Florida. The Gulf Stream Extension Region shows
13 the largest bias difference between the AVHRR-only and the AMSR+AVHRR where the
14 AMSR+AVHRR bias is larger than AVHRR-only. This region usually has the most cloud cover
15 of the three Gulf Stream Regions and hence shows the strongest impact from using or not using
16 AMSR data.

17 The fact that AMSR+AVHRR analysis has a larger bias than AVHRR-only in the Gulf
18 Stream Extension region may be due to bad in situ data. In winter, any bad in situ data would be
19 more likely to be offset by an analysis that used AMSR. An example of a bad buoy just outside
20 the Gulf Stream Extension Region was found near 38°N and 63°W in January 2007 (see Fig. 10
21 from Reynolds et al., 2010). That figure shows a bull's eye in an AATSR-only analysis but not in
22 the AMSR+AVHRR analysis. The problem of bad data can of course occur in both satellite and

1 in situ data. The comparison of different SST analyses is a good way to detect data problems
2 because data are handled differently in each analysis product.

3 In the Aleutians Region, the RTG-HR analysis has its strongest bias. Individual maps
4 showed the RTG-HR had negative biases in the Aleutians and near Iceland in early 2007. In the
5 RTG-HR (and AVHRR-only and AMSR+AVHRR), sea ice coverage is converted to SSTs by
6 climate regression (Reynolds et al. 2007). If the sea ice coverage were too large, the generated
7 SSTs would be too cold. Thus, negative biases in the Aleutians may be related to sea-ice
8 coverage.

9 To investigate the biases in more detail, daily regional average analysis minus buoy
10 differences were computed and temporally smoothed by a 13-day triangular filter. The smoothed
11 differences are plotted in Fig. 8 for the Gulf Stream East Coast and Aleutians Regions. The
12 differences for the Gulf Stream Region show large positive biases for the RSS analysis and large
13 negative biases for the RTG-HR analyses. Furthermore, the OSTIA analysis shows positive
14 biases in the first few months of 2008. In the Aleutians Region, the RTG-HR analysis is more
15 than 2°C colder than the buoys in the winter of 2007. The RTG-HR cold difference also occurred
16 in December 2006 (not shown). The simulated SSTs derived from sea ice and used in the
17 AVHRR-only and AMSR+AVHRR analyses did not lead to negative differences.

18

19 c. *Frequency Spectra*

20 Frequency spectra were computed at each buoy location from the buoy and analysis time
21 series. The individual spectra were averaged over each region. Figure 9 shows the frequency

1 spectra for 3 regions. All spectra shown here are 'red' with the spectral variance decreasing by
2 more than 3 orders of magnitude from the lowest frequency (0.007 cpd) to the highest frequency
3 (0.5 cpd). In Fig. 9 (top), the Gulf Stream East Coast Region, all spectra agree with each other
4 within the confidence limits at low frequencies (< 0.02 cpd). At middle and high frequencies, the
5 buoy spectrum has the largest variance followed by the RSS and NCODA spectra and then by
6 the other analyses. The RTG-HR has the lowest variance between 0.08 and 0.2 cpd. At the
7 highest frequencies (> 0.3 cpd) the AVHRR-only analysis has the lowest variance. At
8 frequencies > 0.1 cpd the buoy spectrum is often above the upper confidence limits for the RSS
9 or NCODA spectra and is always above the confidence limits for the other analyses. These
10 differences between buoys and analyses suggest that all of the analyses underestimate daily SST
11 variability in high gradient regions such as this region of the Gulf Stream.

12 Figure 9 (middle) shows the frequency spectra in the Aleutians Region. At low
13 frequencies (< 0.02 cpd) and at the highest frequencies, the RTG-HR significantly differs from
14 the other analyses and the buoys at the 95% confidence limit. This difference is attributable to
15 the winter bias offset shown in the bottom panel of Fig. 8. At middle frequencies (between 0.02
16 and 0.2), the RSS and RTG-HR analyses have significantly greater variability than the buoys and
17 the other analyses. In addition, the RTG-HR has highest variability at the highest frequencies
18 while the AVHRR-only has the lowest. These high frequency differences are significant and
19 indicate that the RTG-HR is too noisy and that the AVHRR-only is too smooth.

20 The RSS differences with respect to other analyses are not due to the use of TMI in the
21 RSS analysis. Reynolds et al. (2010) shows that the use of TMI provides only modest analysis
22 improvements because TMI coverage is limited to between 38°S and 38°N . However, problems

1 with small-scale noise are evident in the RSS SST fields at all latitudes. The differences are
2 evidently due primarily to the use of the very high-resolution MODIS data in the RSS analysis.

3 Figure 9 (bottom) shows the frequency spectra in the Western Tropical Pacific Region.
4 All spectra agree with each other within the confidence limits at low frequencies (< 0.02 cpd).
5 However, the RSS analysis has significantly larger variance than the other spectra at middle and
6 high frequencies; the RSS SST variance over these frequencies is roughly half an order of
7 magnitude larger than any of the other SST spectra. A similar RSS difference occurs in other
8 tropical regions (Tropical Atlantic and Eastern Tropical Pacific) and is the most dramatic
9 difference among the analyses. The RSS difference is consistent with the wavenumber spectral
10 analysis in Section 4 and the maps in Section 3, which clearly indicate that the RSS analysis
11 needs more spatial smoothing to remove small-scale noise.

12

13 *d. Cross Correlations*

14 Because the spectra are 'red' as shown in Fig 9, the correlations between buoys and
15 analyses will be dominated by the lowest frequencies. The correlations presented here were
16 therefore computed from filtered time series. The filtering consisted of a half-power cutoff
17 frequency of 0.2 cpd (a 5 day period) to separate the low- and high-frequency bands. Cross
18 correlations were computed between the buoys and analysis time series for each region. The
19 average time series was formed by concatenating (in the same order) the individual buoy and
20 analysis time series at each buoy location.

1 The buoy-to-analysis correlations for each region are shown in Fig. 10 for the two
2 frequency bands. The low frequencies (upper panel, < 0.2 cpd) all show correlations above 0.57.
3 The two analyses with the lowest correlations are the RSS (lowest for the Gulf Stream East Coast
4 Region) and RTG-HR (lowest for the Aleutians Region). If the RSS and RTG-HR correlations
5 are excluded, all other correlations exceed 0.80.

6 The high-frequency correlations (lower panel, > 0.2 cpd) are much lower and show more
7 differences among analyses. The NCODA correlations are the highest (between 0.70 and 0.86);
8 the analyses with the next highest correlations vary with region among the AVHRR-only,
9 AMSR+AVHRR and OSTIA, with OSTIA more often better correlated with the buoy
10 observations. The correlations for RTG-HR and RSS are almost always lower than for the other
11 products except in the Gulf Stream Extension Region, where the RTG-HR has a slightly higher
12 correlation than the AMSR+AVHRR analysis. The AVHRR-only and AMSR+AVHRR
13 correlations are very similar (within 0.10) except in the Gulf Stream Extension Region where the
14 AVHRR-only is higher than the AMSR+AVHRR (0.61 and 0.37, respectively). The difference
15 may be related to the cloud cover in this region. If the AVHRR data are restricted due to clouds,
16 the buoy data will be relatively more important in the AVHRR-only analysis than the
17 AMSR+AVHRR analysis. Thus, seasonal changes in cloud cover may impact the correlations.
18 Note, however, that the quality of the AVHRR-only SST analysis can be expected to degrade
19 away from the immediate vicinity of the buoys during periods of persistent cloud cover.

20 To examine the seasonal dependence of the high-frequency correlations, the correlations
21 were recomputed for the months of December, January and February (DJF) and for June, July
22 and August (JJA), as shown in Fig. 11. Outside of the two tropical Pacific regions, correlations

1 were generally higher for JJA than for DJF. The differences in the JJA correlations compared
2 with the DJF correlations ranged from -0.15 to 0.40. The regions with correlation changes > 0.2
3 were the Gulf Stream East Coast, Gulf Stream Extension, UK Ireland, Aleutians and N. America
4 West Coast Regions. These regions are all mid-latitude regions where winter seasonal cloud
5 cover restricts IR retrievals. Furthermore, SST gradients are reduced in summer in most regions.
6 For example, the colder shelf water during winter in the Gulf Stream region (Fig. 1) is usually
7 not present in summer. Thus, it is easier to "fill-in" any missing data in summer analyses and that
8 process enhances the agreement between analyses and buoys. The large DJF correlation
9 difference between AMSR+AVHRR and AVHRR-only in the Gulf Stream Extension became
10 almost the zero in JJA. This difference again suggests that clouds may introduce seasonal
11 variations of the resolution of SST in the AVHRR-only analysis.

12

13 **6. Conclusions**

14 Six different SST analyses have been compared with each other and with buoy data for
15 the two-year period 2007-2008. As summarized in Section 2 and Table 1, the analyses are:
16 AVHRR-only, AMSR+AVHRR, NCODA, RSS, RTG- HR and OSTIA with spatial grid sizes of
17 $1/4^\circ$, $1/4^\circ$, $1/9^\circ$, $1/11^\circ$, $1/12^\circ$ and $1/20^\circ$, respectively. All analyses used differing sets of satellite
18 data. In addition, all analyses except RSS used in situ data. Except for the AVHRR-only and
19 AMSR+AVHRR pair of analyses, the analysis procedures and weighting functions differ for all
20 of the products. Thus, it is not surprising that the analyzed SSTs also differ. An example off the
21 coast of South Carolina showed SST differences that can exceed 5°C in winter. In this example,

1 the OSTIA and RSS analyses do not clearly show the expected cold coastal water. In other
2 regions and time periods, there are large differences among the various analyses and the best
3 analysis is more difficult to determine.

4 To assess the feature resolution capability of the various SST products, wavenumber
5 spectra were computed at three different locations. These results clearly indicate that the RSS
6 analysis is much noisier and the RTG-HR analysis is much smoother than the other analyses. It
7 was shown that the feature resolution is always coarser than the grid spacing. A perhaps
8 surprising result of the wavenumber spectra is that the spatial resolution for each SST product in
9 general varies geographically and temporally (summer vs. winter). It is therefore not possible to
10 assign a single spatial resolution to any of the SST products considered here.

11 Further comparisons were made using collocated buoys for ten regions from time series
12 using frequency spectral analysis and cross correlations of low- and high-pass filtered time series
13 from the buoy data and the six SST analyses. These comparisons also showed that RSS is too
14 noisy in the tropics. They also revealed that RTG-HR had winter biases in the Aleutians Region
15 during January and February 2007. The correlation results showed that buoy-to-analysis
16 correlations at high frequencies (> 0.2 cpd) were best for the NCODA and OSTIA analyses and
17 worst for the RTG-HR and RSS analyses. The high correlations suggest that NCODA, and to a
18 somewhat lesser extent, OSTIA were strongly tuned locally to buoy data, where they exist.

19 It is important to distinguish between the grid spacing and the feature resolution of an
20 SST analysis. The grid spacing defines the smallest possible features that could be resolved in an
21 analysis. A grid scale that is unnecessarily smaller than the features that are actually resolved by
22 the analysis is computationally inefficient. Moreover, such mismatch between grid spacing and

1 feature resolution conveys a false impression of the resolution capability to the casual user who
2 often misinterprets grid resolution as feature resolution. The feature resolution is determined by
3 analysis parameters such as error correlation scales and signal-to-noise ratio, and can be limited
4 by the resolution of the input observations (e.g., the footprint sizes of about 50 km for MW, 4-9
5 km for AVHRR and 1 km for MODIS) and by the sampling density over the temporal period of
6 the analysis. In the examples shown here, the OSTIA analysis has the smallest grid size and yet
7 the feature resolution is not significantly smaller than the other analyses. If the analysis
8 procedure does not incorporate sufficient smoothing, as in the case of the RSS analysis, the
9 analysis will contain many small-scale features that are artifacts of small-scale measurement
10 noise rather than signal.

11 Another important factor is the impact of seasonal variations in cloud cover on an SST
12 analysis. Consider, for example, a region with 1 km IR data and 50 km MW data. During cloudy
13 periods the IR data will be limited while the MW data will not be impacted (except in the case of
14 rain). Thus, any analysis which attempts to obtain the highest resolution possible based on IR
15 data unavoidably degrades this resolution when the IR data are missing or the coverage is
16 reduced. This change in IR coverage can result in apparent temporal inhomogeneity in the small-
17 scale variance that could wrongly be interpreted as real and may be problematic for some
18 applications.

19 An additional issue is that there is generally a strong correlation between time and space
20 scales; small features are less persistent than large features. If the analysis procedure attempts to
21 resolve very small features in the SST field (e.g., the RSS analysis), there may be insufficient
22 high-resolution data during cloudy periods, thus resulting in noise in the SST analysis. If the

1 smoothing in the analysis procedure is too large (e.g., the RTG-HR analysis), the SST fields will
2 be unnecessarily smooth. One possible solution to this dilemma is to produce an analysis with
3 two analysis stages. In the first stage, a coarse resolution SST analysis is produced based on
4 combined MW and IR data similar to that described by Reynolds et al. (2007). In the second
5 stage, a high-resolution analysis is produced with a finer grid spacing using only the available IR
6 data; MW and in situ data are not be used directly in the high-resolution analysis. This procedure
7 could improve the low-resolution product when sufficient IR data are available. In regions of
8 sparse IR data, the high-resolution product would damp toward the low-resolution product. An
9 important feature of such a 2-stage analysis is that it must include information about the
10 coverage of the IR data so that users can assess when and where small-scale features can be
11 adequately resolved in the second stage analysis.

12 The AVHRR-only analysis is uniquely useful for climate studies because it is the only
13 daily SST analysis that extends back to September 1981. It was shown in section 3 that inclusion
14 of AMSR data can actually reduce the resolution of the combined AMSR and AVHRR analysis
15 compared with the AVHRR-only analysis during cloud-free time periods. When there is
16 extensive cloud cover, however, as often occurs at midlatitudes in the wintertime, AMSR
17 improves the AMSR+AVHRR analysis over AVHRR-only. These results indicate that spatial
18 and temporal variations in the satellite data that are incorporated in an SST analysis (e.g., AMSR
19 vs. AVHRR or MODIS) can impact the resolution of the resulting SST fields and result in
20 artificial spatial and temporal variability of the apparent scales of features in the SST field. This
21 should be kept in mind when using the SST analyses to investigate climate variability.

22

1 *Acknowledgments.* We thank Qingtao Song for help producing the wavenumber spectra in
2 Figure 5. DBC was supported by NASA Contract 1283973 and 1283976 from the Jet Propulsion
3 Laboratory for funding of Ocean Vector Winds Science Team Activities, and by Award
4 NA03NES4400001 to Oregon State University from NOAA. We are grateful to NCDC and the
5 NOAA Office of Global Programs, which provided partial support for this work. The graphics
6 for many of the figures were computed using the Grid Analysis and Display System (GrADS)
7 (<http://grads.iges.org/grads>), Center for Ocean-Land-Atmosphere Studies. We also appreciate the
8 help of two NOAA reviewers (Mike McPhaden and Ken Casey) and two anonymous reviewers.

1 **References**

- 2 Bourlès, B., and Coauthors, 2008: The Pirata Program: History, Accomplishments, and Future
3 Directions. *Bull. Amer. Meteor. Soc.*, **89**, 1111–1125.
- 4 Castelao, R. M., T. P. Mavor, J. A. Barth, and L. C. Breaker, 2006: Sea-surface temperature
5 fronts in the California Current System from geostationary satellite observations. *J.*
6 *Geophys. Res.*, **111**, C09026, doi:10.1029/2006JC003541.
- 7 Chelton, D. B., and F. J. Wentz, 2005: Global microwave satellite observations of sea-surface
8 temperature for numerical weather prediction and climate research. *Bull. Amer. Meteor.*
9 *Soc.*, **86**, 1097-1115.
- 10 Chelton, D. B., R. A. de Szoeke, M. G. Schlax, K. El Naggar and N. Siwertz, 1998:
11 Geographical variability of the first-baroclinic Rossby radius of deformation. *J. Phys.*
12 *Oceanogr.*, 28, 433–460.
- 13 Cummings, J. A., 2005: Operational multivariate ocean data assimilation, *Q. J. R. Meteorol.*
14 *Soc.*, **131**, 3583-3604.
- 15 Donlon, C. and others, 2007: The Global Ocean Data Assimilation Experiment High-resolution
16 Sea Surface Temperature Pilot. *Bull. Amer. Meteor. Soc.*, **88**, 1197-1213.
- 17 Donlon, C., M. Martin, J. Stark, J. Roberts-Jones and E. Fiedler, 2009: The Operational Sea
18 Surface Temperature and Sea Ice Analysis (OSTIA). *Remote Sensing of Environment* (in
19 review).

- 1 Gemmill, William, Bert Katz and Xu Li, 2007: Daily Real-Time Global Sea Surface
2 Temperature - High Resolution Analysis at NOAA/NCEP. NOAA / NWS / NCEP /
3 MMAB Office Note Nr. 260, 39 pp (Available at: <http://polar.ncep.noaa.gov/sst/>)
- 4 Gentemann, C. L., C. J. Donlon, A. Stuart-Menteth and F. J. Wentz, 2003. Diurnal Signals in
5 Satellite Sea Surface Temperature Measurements, *Geophys. Res. Lett.*, **30**, 1140,
6 doi:10.1029/2002GL016291
- 7 May, D. A., M. M. Parmer, D. S. Olszewski and B. D. McKenzie, 1998: Operational
8 processing of satellite sea surface temperature retrievals at the Naval Oceanographic
9 Office. *Bull. Amer. Met. Soc.*, **79**, 397-407.
- 10 McPhaden, M. J., and Coauthors, 1998: The Tropical Ocean-Global Atmosphere (TOGA)
11 observing system: A decade of progress. *J. Geophys. Res.*, **103**, 14 169–14 240.
- 12 Reynolds, R. W. and T. M. Smith, 1994: Improved global sea surface temperature analyses using
13 optimum interpolation. *J. Climate*, **7**, 929-948.
- 14 Reynolds, R. W., N. A. Rayner, T. M. Smith, D. C. Stokes and W. Wang, 2002: An improved in
15 situ and satellite SST analysis for climate. *J. Climate*, **15**, 1609-1625.
- 16 Reynolds, R. W., T. M. Smith, C. Liu, D. B. Chelton, K. S. Casey, and M. G. Schlax, 2007:
17 Daily high-resolution blended analyses for sea surface temperature. *J. Climate*, **20**, 5473-
18 5496.
- 19 Reynolds, R.W., C. L. Gentemann and G. K. Corlett, 2010: Evaluation of AATSR and TMI
20 Satellite SST Data. *J. Climate*, **23**, 152–165.

1 Thiébaux, J., E. Rogers, W. Wang and B. Katz, 2003: A new high-resolution blended real-time
2 global sea surface temperature analysis. *Bull. Amer. Meteor. Soc.*, **84**, 645-656.

3 Worley, S. J., S. D. Woodruff, R. W. Reynolds, S. J. Lubker, and N. Lott, 2005: ICOADS release
4 2.1 data and products. *Int. J. Climatol.*, **25**, 823–842.

5

1 **List of Figures**

2 FIG 1. Daily SST fields for 1 January 2007 from the six analyses considered in this study. Note in
3 particular the differences near the South Carolina Coast (roughly 33°N, 80°W). The contour
4 interval is 1°C.

5 FIG 2. Daily SST gradient magnitudes for 1 January 2007 from the six SST analyses. Gradients
6 are computed as centered differences only if all four of the nearest east/west and north/south
7 neighbors are present. The contour interval is 2°C/100 km.

8 FIG 3. Daily SST fields for 1 January 2007 from the six SST analyses. Small-scale features are
9 most evident in RSS and RTG-HR is the smoothest. The shading interval is 0.5°C.

10 FIG 4. SST gradient magnitudes for 1 September 2008 from the six SST analyses. Note the
11 coastal gradients due to upwelling. Gradients are computed as in Fig 2. The shading interval is
12 1°C/100 km.

13 FIG 5. Zonal wavenumber spectra for January 2007 (left) and July 2007 (right) for three regions
14 of the World Ocean: the Agulhas Return Current (45°E to 85°E, 47°S to 38°S), the Kuroshio
15 Extension (150°E to 150°W, 30°N to 45°N) and the western tropical Pacific (150°E to 160°W, 5°S
16 to 10°N). For each region, wavenumber spectra were computed from daily averaged SST fields
17 in each month along each latitude of grid points within the specified domain. These individual
18 spectra were then ensemble averaged over the latitudes and the 31 days of each month. The color
19 key for the six SST products is shown in the upper left panel.

20 FIG 6. Location of 1/4° grid points with daily buoy SST observations for at least 90% of the time
21 period: 1 January 2007 – 31 December 2008. Ten regions are indicated in numerical order: Gulf

1 of Mexico (GM), Gulf Stream Florida (GSF), Gulf Stream East Coast (GSEC), Gulf Stream
2 Extension (GSE), UK/Ireland (UKI), Tropical Atlantic (TA), Aleutians (AL), North America
3 West Coast (NAWC), Tropical West Pacific (TWP) and Tropical East Pacific (TEP).

4 FIG 7. RMS of the bias of the monthly average buoy - analysis difference for the six analyses
5 and ten regions (see Fig. 6). The largest biases occur in the Gulf Stream Regions for all analyses.
6 The buoy - NCODA RMS differences are the lowest for each region; the RSS and RTG-HR
7 differences are generally larger than the others.

8 FIG 8. Daily biases of the buoy - analysis difference for the six analyses for the Gulf Stream East
9 Coast Extension Region (top) and the Aleutians Region (bottom). A 13-day triangular weighted
10 running average was applied to the time series.

11 FIG 9. Average frequency spectra for the buoys and the six analyses at the buoy locations shown
12 in Fig. 6 for the Gulf Stream East Coast Region (top), Aleutians Region, (middle) and Tropical
13 West Pacific Region (bottom). The spectra are computed at each buoy location and averaged
14 over the region. Note the large RTG-HR difference from the other spectra in the Aleutians, and
15 the high values for the RSS analysis for frequencies > 0.02 cpd.

16 FIG 10. Correlations for low frequencies (< 0.2 cpd, top panel) and high frequencies (> 0.2 cpd,
17 bottom panel) computed over the 2007-2008 time period for the six analyses and ten regions (see
18 Fig. 6). Note that the NCODA – buoy high frequency correlations are the largest.

19 FIG 11. Correlations for high frequencies (> 0.2 cpd) for December, January and February (top)
20 and June, July and August (bottom) computed over the 2007-2008 time period for the six
21 analyses and ten regions (see Fig. 6).

1

2 **TABLE 1.** Summary of the six analyses sorted by increasing equatorial grid spacing. All analyses
 3 except the RTG-HR product are available at
 4 <ftp://podaac.jpl.nasa.gov/pub/GHRSST/data/L4/GLOB/>. In situ observations are SSTs from
 5 ships and buoys, except for NCODA which also includes also includes in situ hydrographic
 6 temperature and salinity profiles.

7

8	Analysis Name	Input Data	Equatorial	Temporal	Start
9			Resolution	Resolution	Date
10					
11	1. AVHRR-only	AVHRR, in situ	28 km (1/4°)	Daily	Sep 1981
12	2. AMSR+AVHRR	AMSR, AVHRR, in situ	28 km (1/4°)	Daily	Jun 2002
13	3. NCODA	AVHRR, in situ,	12 km (1/9°)	6 Hour	Oct 2005
14		altimeters, atmospheric forcing			
15					
16	4. RSS	AMSR, TMI, MODIS	10 km (1/11°)	Daily	Aug 2005
17	5. RTG-HR	AVHRR, in situ	9 km (1/12°)	Daily	Sep 2005
18	6. OSTIA	AVHRR, AMSR, TMI,	6 km (1/20°)	Daily	Mar 2006
19		AATSR, SEVIRI, in situ			
20					

21

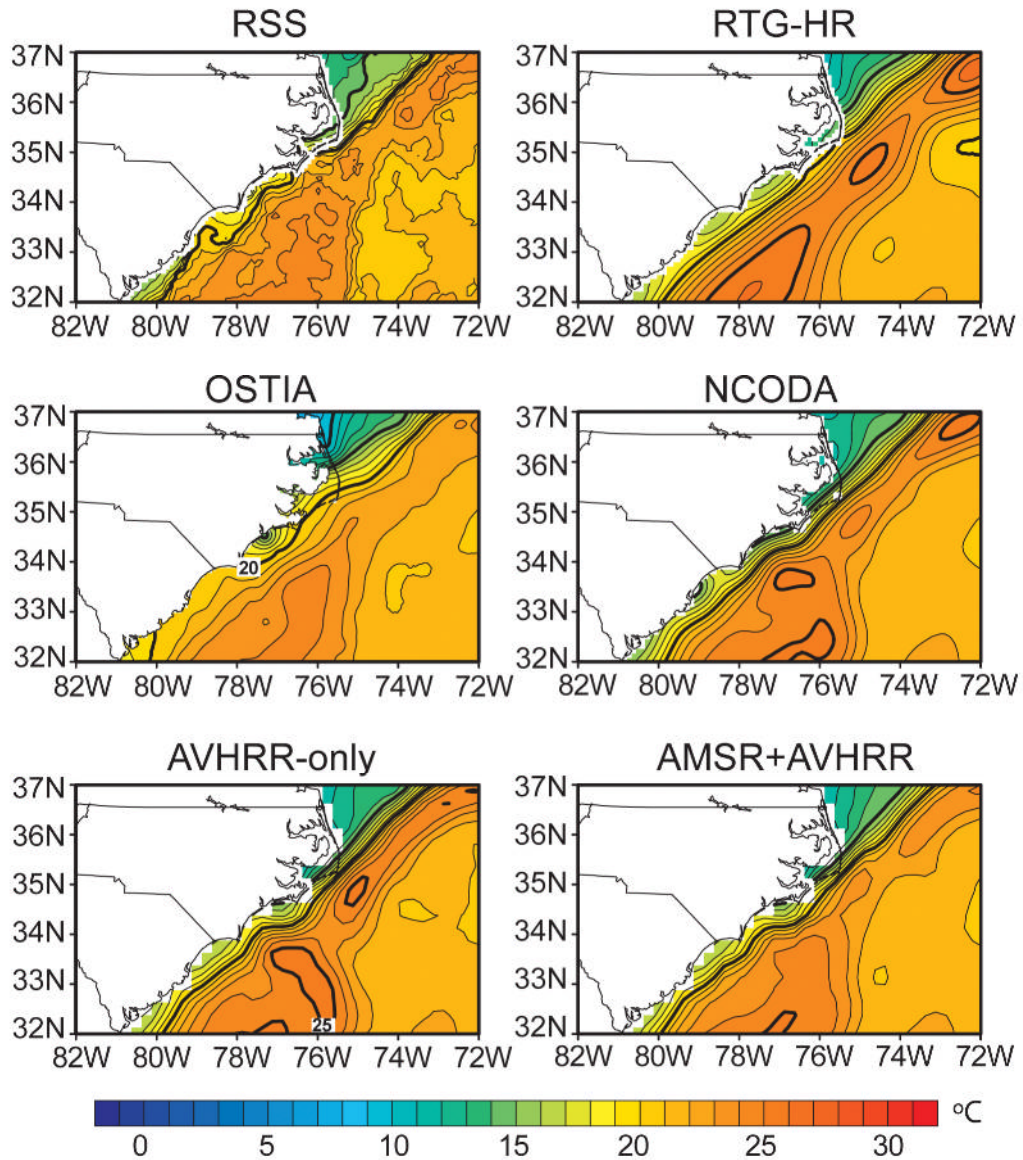


FIG 1. Daily SST fields for 1 January 2007 from the six analyses considered in this study. Note in particular the differences near the South Carolina Coast (roughly 33°N, 80°W). The contour interval is 1°C.

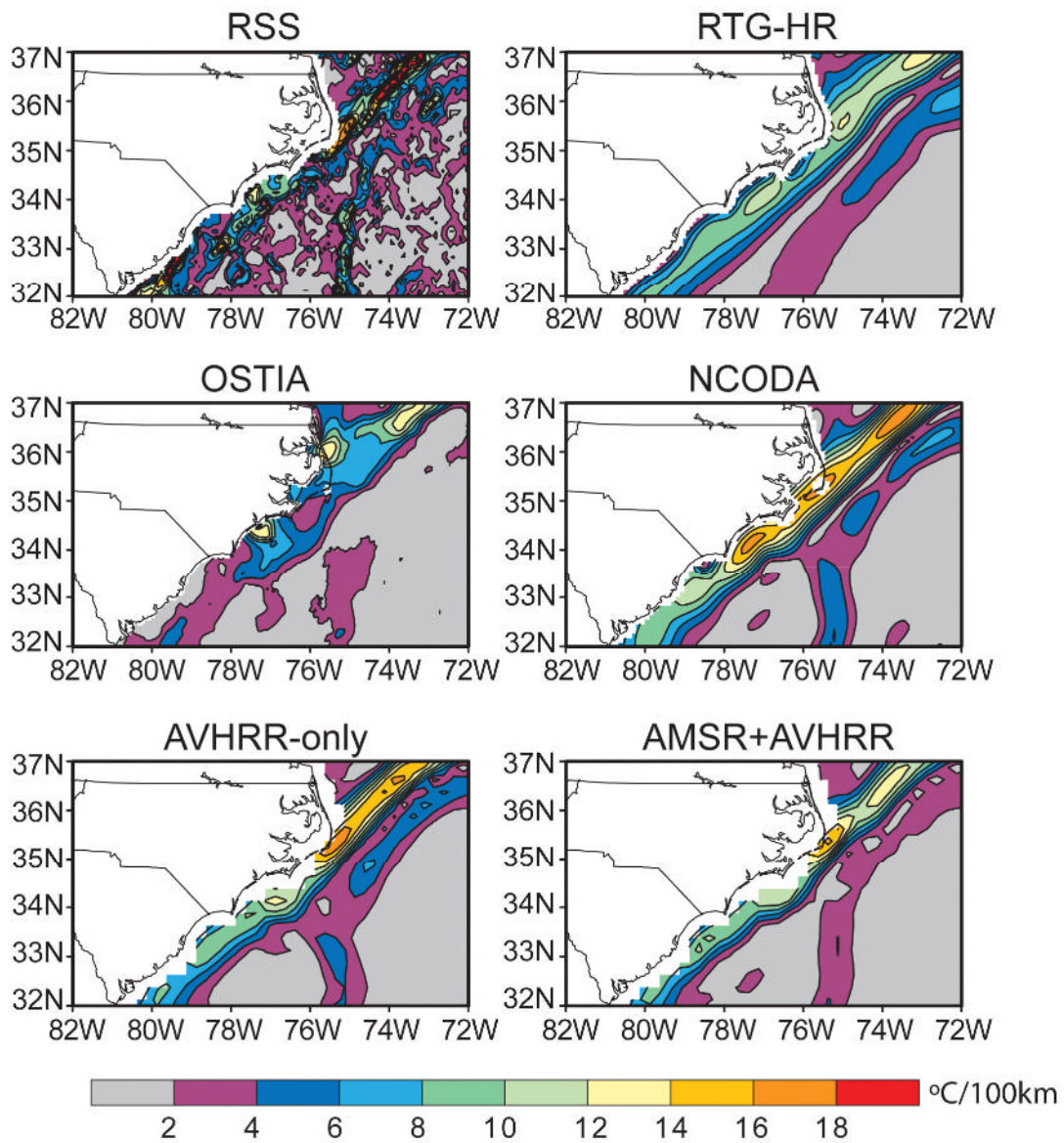


FIG 2. Daily SST gradient magnitudes for 1 January 2007 from the six SST analyses. Gradients are computed as centered differences only if all four of the nearest east/west and north/south neighbors are present. The contour interval is $2^{\circ}\text{C}/100\text{ km}$.

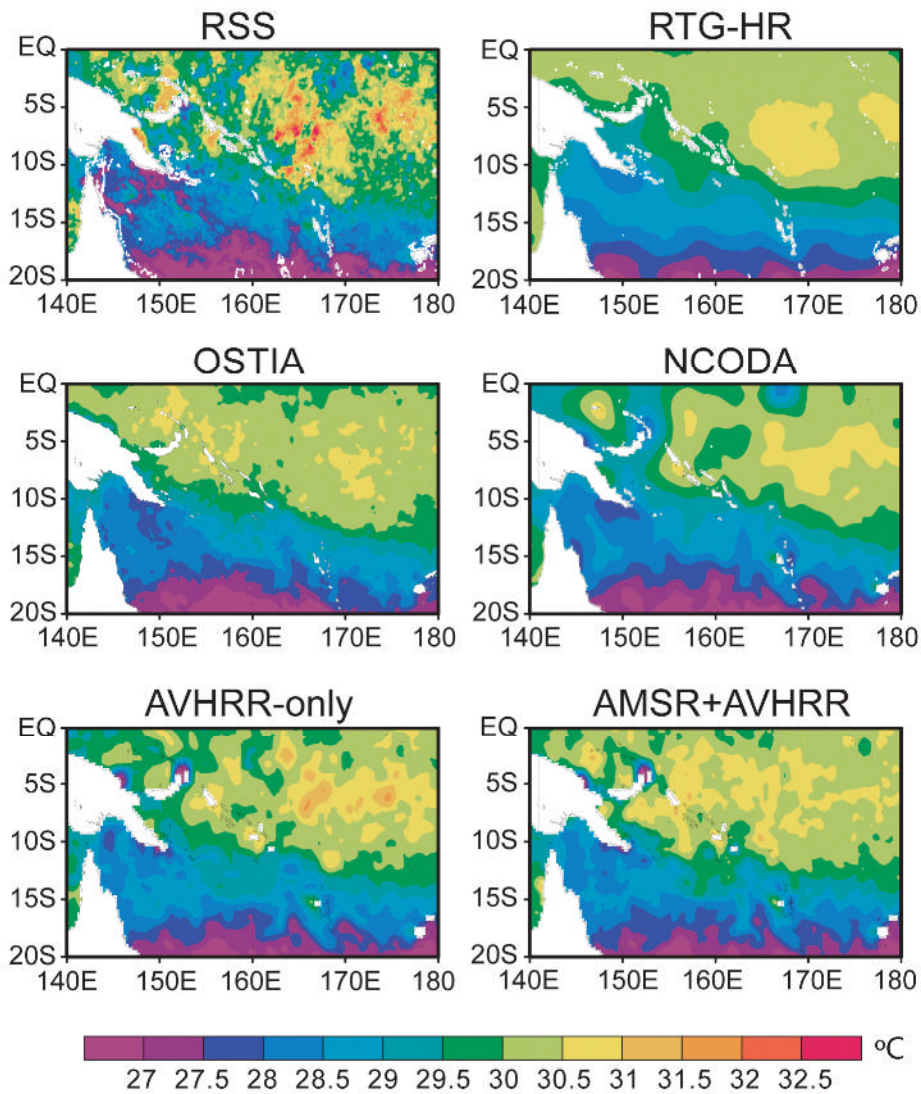


FIG 3. Daily SST fields for 1 January 2007 from the six SST analyses. Small-scale features are most evident in RSS and RTG-HR is the smoothest. The shading interval is 0.5°C.

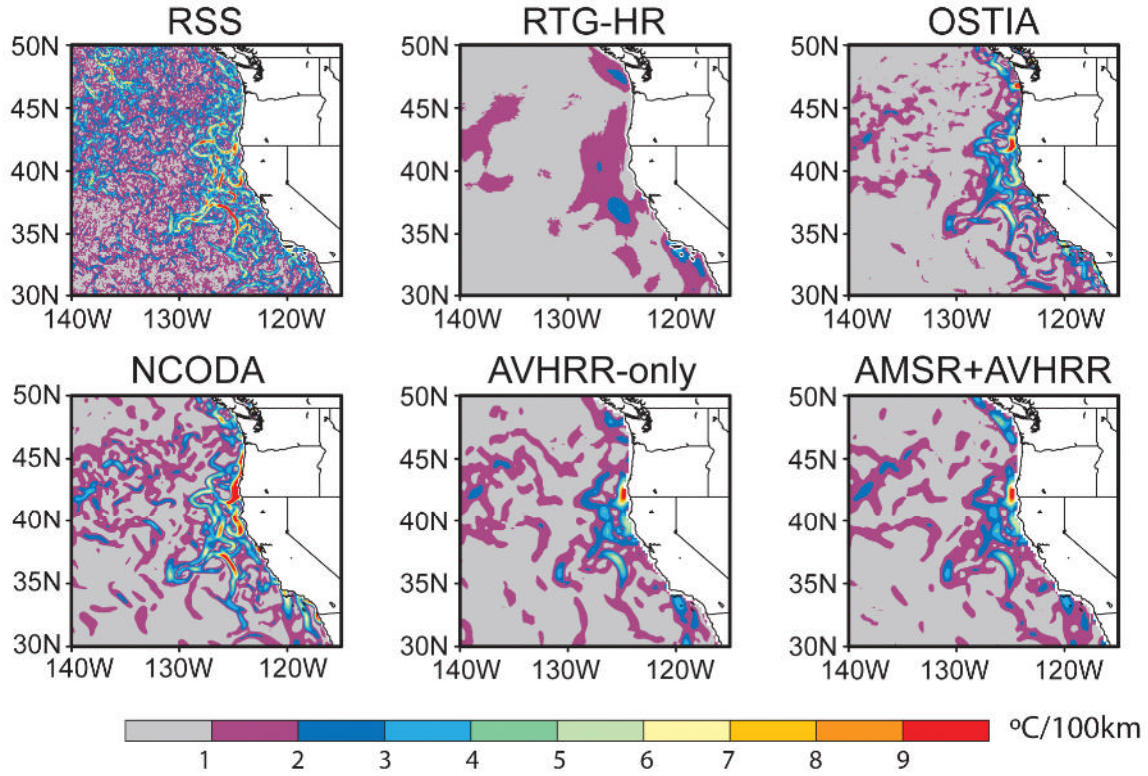


FIG 4. SST gradient magnitudes for 1 September 2008 from the six SST analyses. Note the coastal gradients due to upwelling. Gradients are computed as in Fig 2. The shading interval is $1^{\circ}\text{C}/100\text{ km}$.

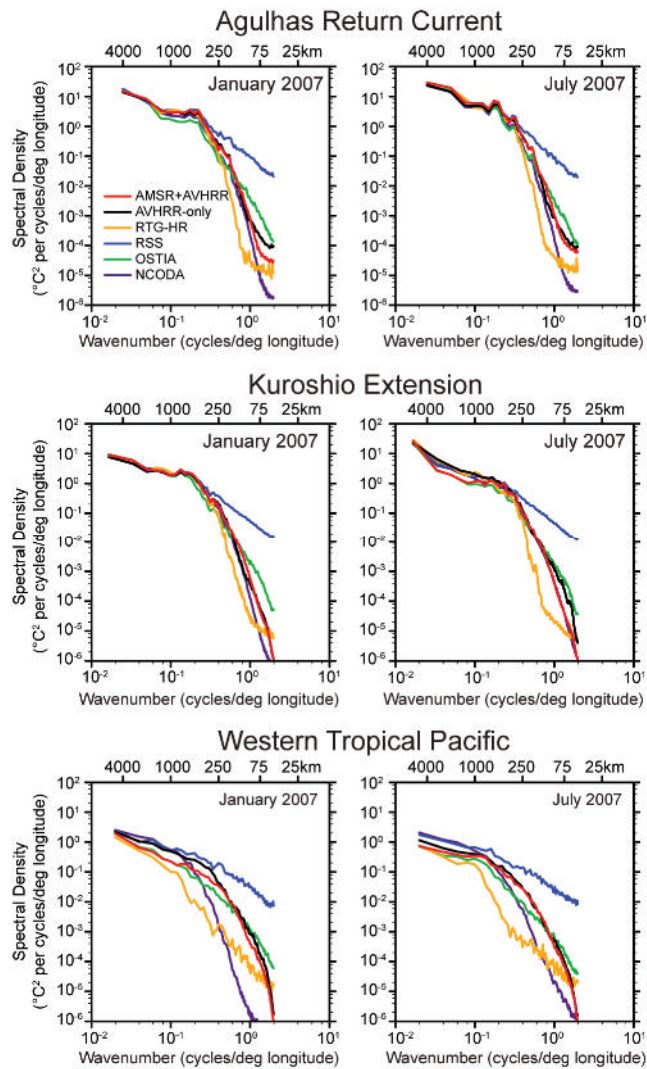


FIG 5. Zonal wavenumber spectra for January 2007 (left) and July 2007 (right) for three regions of the World Ocean: the Agulhas Return Current (45°E to 85°E, 47°S to 38°S), the Kuroshio Extension (150°E to 150°W, 30°N to 45°N) and the western tropical Pacific (150°E to 160°W, 5°S to 10°N). For each region, wavenumber spectra were computed from daily averaged SST fields in each month along each latitude of grid points within the specified domain. These individual spectra were then ensemble averaged over the latitudes and the 31 days of each month. The color key for the six SST products is shown in the upper left panel.

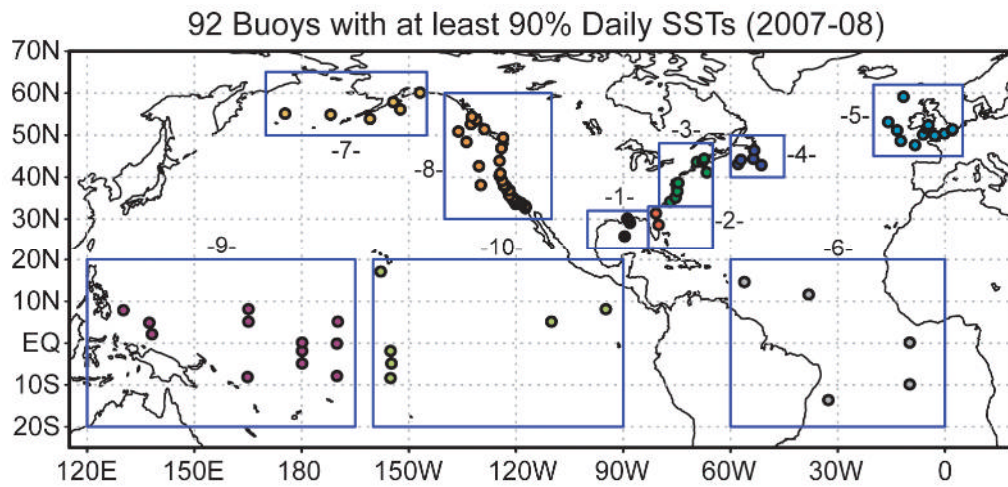


FIG 6. Location of $1/4^\circ$ grid points with daily buoy SST observations for at least 90% of the time period: 1 January 2007 – 31 December 2008. Ten regions are indicated in numerical order: Gulf of Mexico (GM), Gulf Stream Florida (GSF), Gulf Stream East Coast (GSEC), Gulf Stream Extension (GSE), UK/Ireland (UKI), Tropical Atlantic (TA), Aleutians (AL), North America West Coast (NAWC), Tropical West Pacific (TWP) and Tropical East Pacific (TEP).

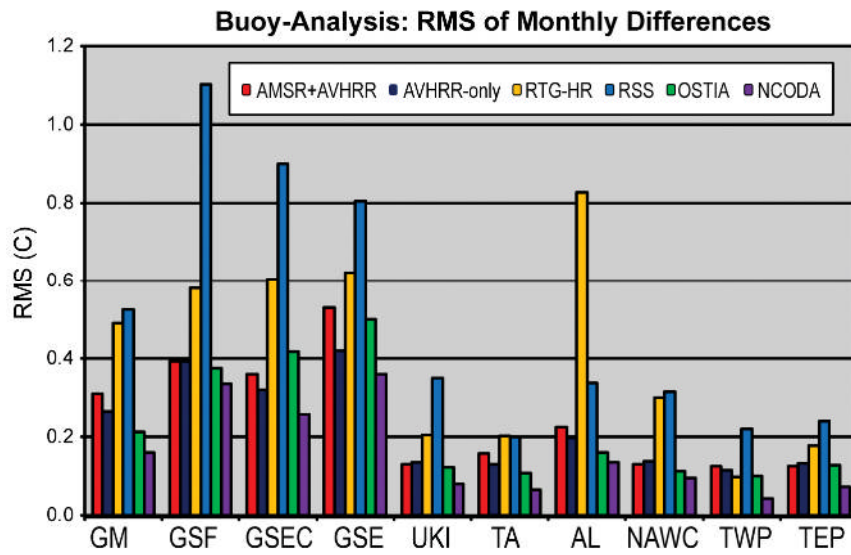


FIG 7. RMS of the bias of the monthly average buoy - analysis difference for the six analyses and ten regions (see Fig. 6). The largest biases occur in the Gulf Stream Regions for all analyses. The buoy - NCODA RMS differences are the lowest for each region; the RSS and RTG-HR differences are generally larger than the others.

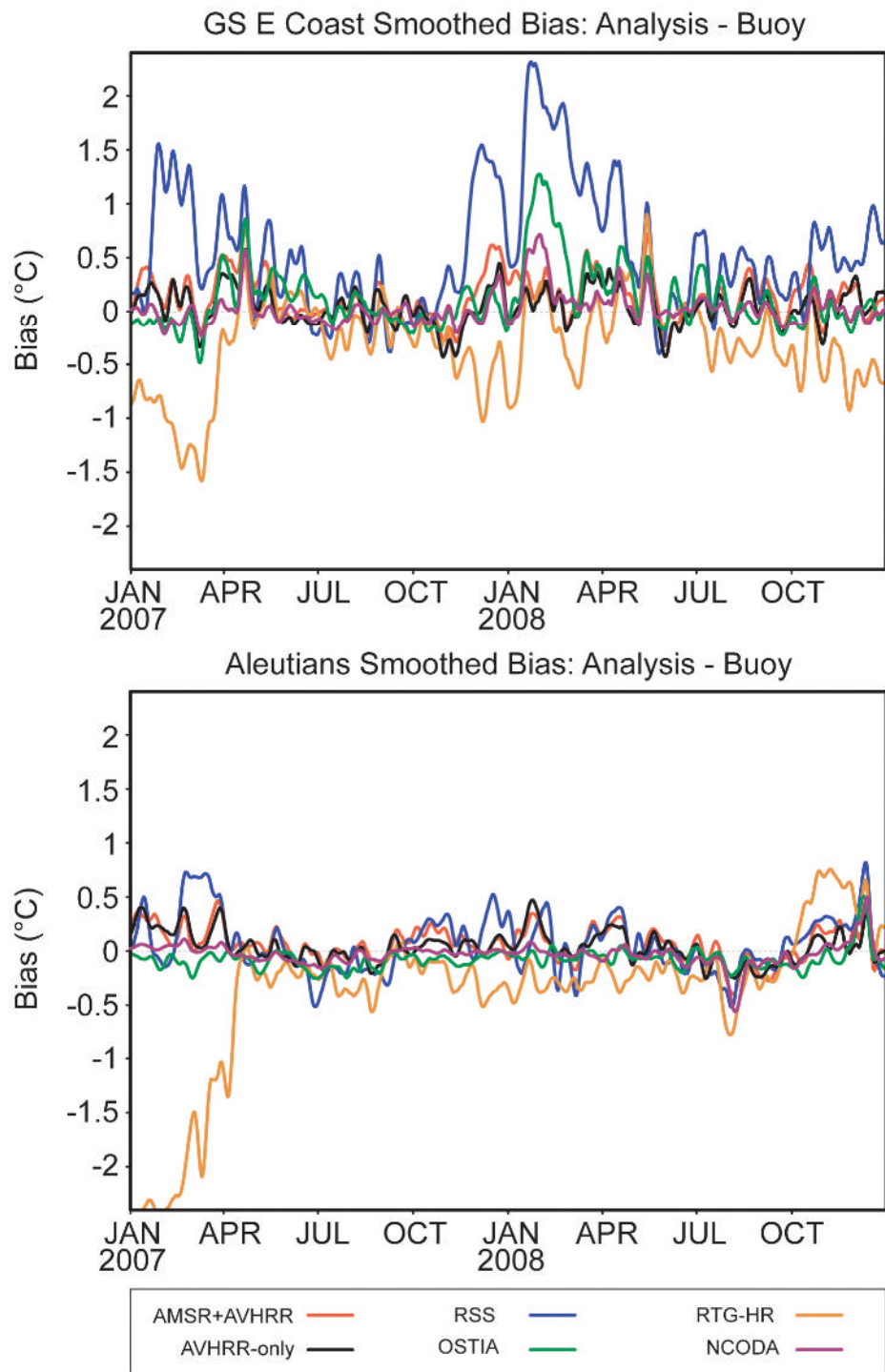


FIG 8. Daily biases of the buoy - analysis difference for the six analyses for the Gulf Stream East Coast Extension Region (top) and the Aleutians Region (bottom). A 13-day triangular weighted running average was applied to the time series.

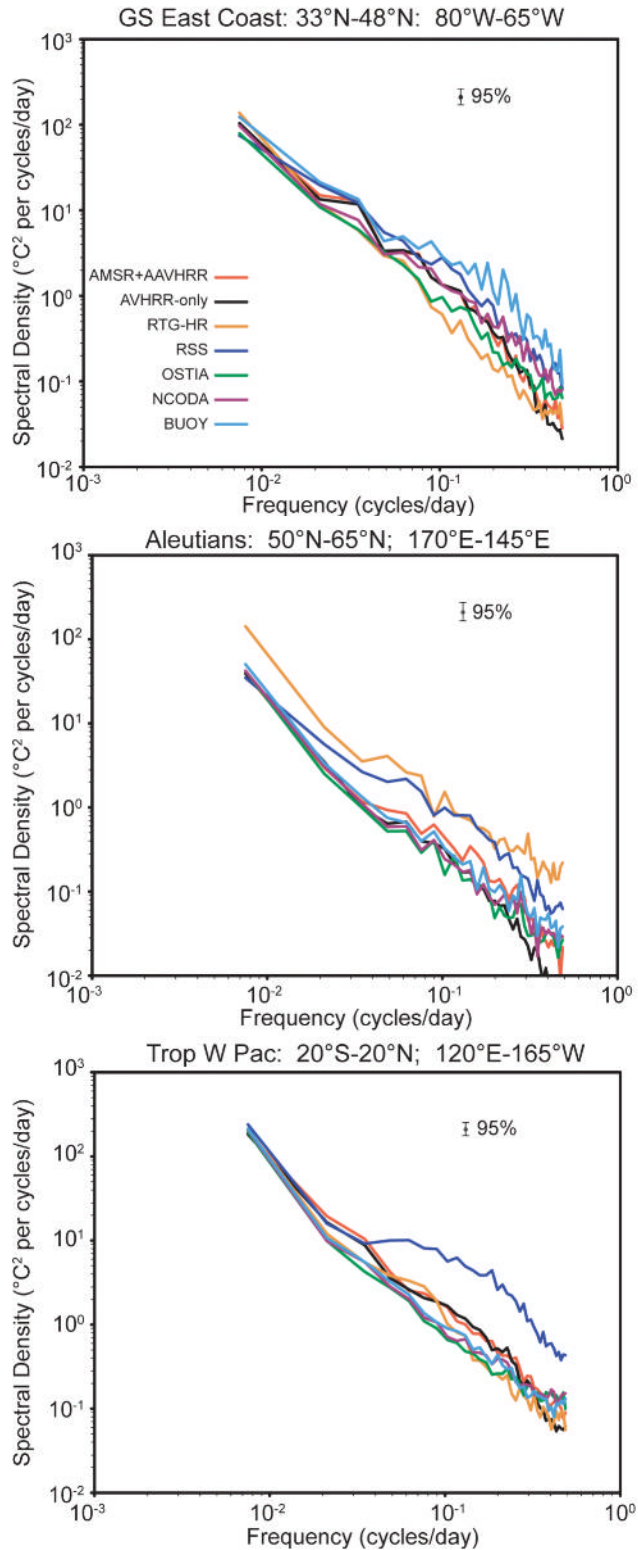


FIG 9. Average frequency spectra for the buoys and the six analyses at the buoy locations shown in Fig. 6 for the Gulf Stream East Coast Region (top), Aleutians Region, (middle) and Tropical West Pacific Region (bottom). The spectra are computed at each buoy location and averaged over the region. Note the large RTG-HR difference from the other spectra in the Aleutians, and the high values for the RSS analysis for frequencies > 0.02 cpd.

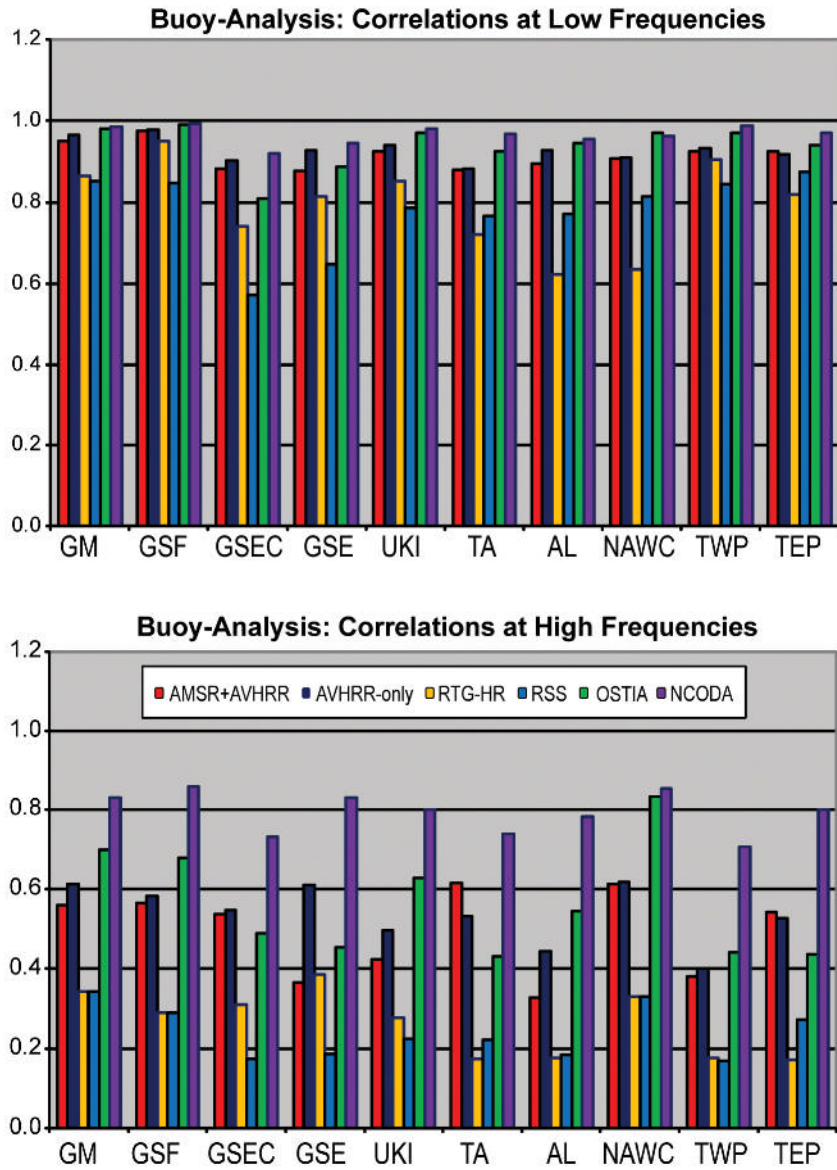


FIG 10. Correlations for low frequencies (< 0.2 cpd, top panel) and high frequencies (> 0.2 cpd, bottom panel) computed over the 2007-2008 time period for the six analyses and ten regions (see Fig. 6). Note that the NCODA – buoy high frequency correlations are the largest.

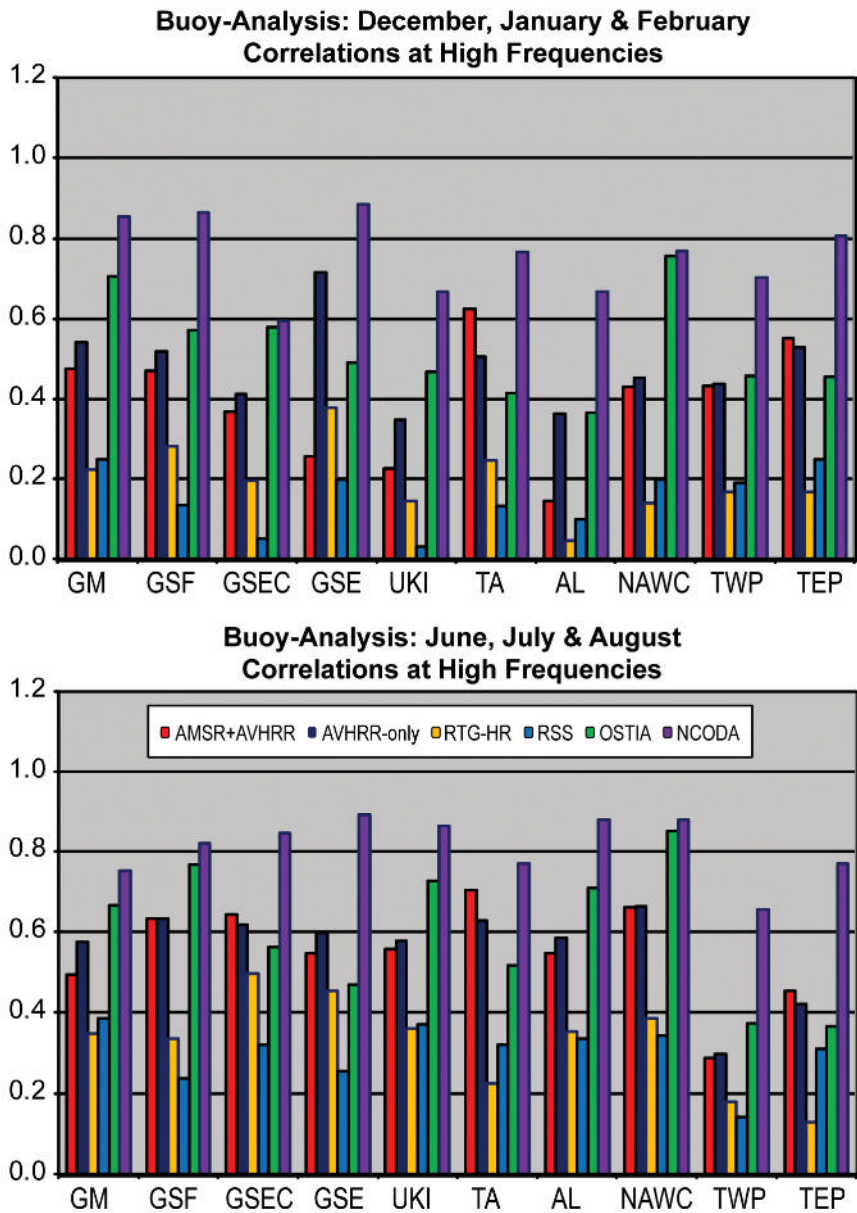


FIG 11. Correlations for high frequencies (> 0.2 cpd) for December, January and February (top) and June, July and August (bottom) computed over the 2007-2008 time period for the six analyses and ten regions (see Fig. 6).